

our cross section for A_2^0 production in Reaction (2) comes out to be $11.6 \pm 1.6 \mu\text{b}$.¹

Several analyses have used an unitarized model to describe the diffractive data in terms of an A_1 resonance in the presence of a Deck background.¹¹ Their results are indicative of the presence of an A_1 resonance of mass ranging between 1300 and 1500 MeV and width of 200–400 MeV. If such a resonance exists, it should be visible in the non-diffractive $1^+(\rho\pi) s$ amplitude (Fig. 4). There is no evidence in our data for a high-mass A_1^0 . The highest upper limit in the interval $m_{3\pi} \leq 1.5$ GeV can be set at 1.3 GeV: $\sigma_{1.3} < 3 \mu\text{b}$, consistent with the cross section expected for an A_1 resonance of this mass.¹⁰ The phase of the $1^+(\rho\pi) s$ wave shows no evidence for a resonant increase at 1.3 GeV, however, the absolute value of the amplitude is too small below $m_{3\pi} = 1.2$ GeV for an accurate measurement. For the A_3^0 , the 1σ upper limit in Reaction (2) is $\sigma_{A_3^0} < 1 \mu\text{b}$.

In conclusion, we have isolated for the first time the wave responsible for the A_4 enhancement: $3^+(g\pi) s$. Within the framework of our analysis, none of the A_1 , A_3 , or A_4 enhancements is associated with the Breit-Wigner type of phase variation which characterizes the well-established resonances such as the A_2 . Also none of the A_1^0 , A_3^0 , or A_4^0 is produced by charge exchange in Reaction (2). Our upper limit for A_1^0 production

at a mass of 1.1 GeV is more than one order of magnitude smaller than the cross section for A_2^0 production in the same process. However, our data do not rule out a higher-mass A_1 , i.e., $m_{A_1} \sim 1.3$ GeV.

This research was supported by the National Science Foundation.

¹C. V. Cautis, Ph.D. thesis, Columbia University, 1977 (unpublished), and Nevis Report No. 221 (unpublished).

²G. Ascoli *et al.*, Phys. Rev. D **7**, 669 (1973).

³Yu. M. Antipov *et al.*, Nucl. Phys. **B63**, 153 (1973).

⁴G. Thompson *et al.*, Phys. Rev. Lett. **32**, 331 (1974); G. Thompson *et al.*, Phys. Rev. D **9**, 560 (1974).

⁵G. Otter *et al.*, Nucl. Phys. **B80**, 1 (1974).

⁶C. Baltay *et al.*, to be published; M. Kalelkar, Ph.D. thesis, Columbia University, 1975 (unpublished), and Nevis Report No. 207 (unpublished); S. Csorna, Ph.D. thesis, Columbia University, 1975 (unpublished), and Nevis Report No. 211 (unpublished).

⁷J. D. Hansen *et al.*, Nucl. Phys. **B81**, 403 (1974).

⁸S. U. Chung and T. L. Trueman, Phys. Rev. D **11**, 633 (1975).

⁹J. Orear, UCRL Report No. UCRL-8417, 1958 (unpublished).

¹⁰H. E. Haber and G. L. Kane, University of Michigan Report No. UM HE 77-9, 1977 (to be published).

¹¹M. G. Bowler *et al.*, Nucl. Phys. **B97**, 227 (1975); J. L. Basdevant and E. L. Berger, ANL Report No. HEP-PR-77-02, 1977 (to be published); R. S. Longacre and R. Aaron, Phys. Rev. Lett. **38**, 1509 (1977).

Study of Heavy-Ion-Induced Reactions on Uranium with Use of Mica Detectors

P. Vater, H.-J. Becker, and R. Brandt

Kernchemie, Philipps-Universität, D-3550 Marburg, Lahnberge, Germany

and

H. Freiesleben^(a)

Fachbereich Physik, Philipps-Universität, D-3550 Marburg, Lahnberge, Germany

(Received 14 February 1977)

Multifragment reactions are directly observed in heavy-ion-induced reactions using mica track detectors in 2π geometry. Sequential fission is found to be the major reaction channel in the reaction 800-MeV $^{84}\text{Kr} + \text{U}$; however, binary decay can still be identified. A small contribution of reactions with four fragments is observed for the first time in ^{84}Kr - and ^{136}Xe -induced reactions with uranium.

Fission at low and moderate excitation energy is essentially a binary decay process. Theoretical arguments have been presented over a long period of time suggesting that ternary fission should be a possible reaction channel too. Fleischer *et al.* describe the discovery of such a decay mode for Ar-induced reactions.¹ The measured

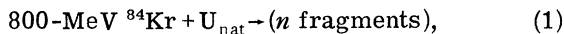
cross section σ_{3F} has always been small: $\sigma_{3F} \leq 0.05\sigma_R$, σ_R being the total reaction cross section.²

Recently, heavy ions like Kr or Xe became available for nuclear reaction studies. A new type of reaction was observed, very often named "strongly damped collision."³ Radiochemical

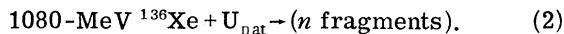
studies on the systems $U + Fe$,⁴ $U + Kr$,⁵ and $U + Xe$ ⁶ confirmed the existence of such a new process. The interaction between the two heavy ions often leads to targetlike and projectilelike fragments, both being excited. In a second step, fission of the targetlike fragment can take place, thus yielding for uranium targets a high cross section for "quasiternary fission"⁴⁻⁶ or "sequential fission"⁷ (the latter term will be used in this contribution).

Here we report on a direct study of reactions with two, three, or four fragments in the exit channel using mica track detectors. Based on the registration threshold for mica we empirically define a "fragment" to be heavier than approximately 30 amu.² We confirm that binary decay is a minor reaction channel and show that sequential fission is the major reaction channel. For the first time, reactions with four fragments (>30 amu) have been observed as a new reaction channel in heavy-ion-induced nuclear reactions on uranium targets.

We studied the reactions



and, in less detail,



The irradiations for Reactions (1) and (2) have been carried out at the linac in Manchester and at the SuperHILAC in Berkeley, respectively. We employed the 2π -geometry mica technique: Mica covered with a thin UF_4 layer is irradiated normal to its surface with approximately 2×10^6 (Kr) cm^{-2} and fragment tracks are made visible by etching. The observed single dots as shown in Fig. 1 are due to individual Kr ions. By counting their number, one can obtain the heavy-ion flux.⁸ Additionally, one observes two-, three-, and four-pronged events due to interactions of heavy ions with the U target nuclei. Thus, we see directly the number of fragments from an individual interaction going into the forward hemisphere of the laboratory system and, to some extent, we can estimate the total number of fragments in the 4π geometry. An exact measurement of track lengths l and angles ξ between tracks and beam direction allows a classification of events as being due to either elastic scattering or nuclear interactions.^{8,9}

From the events attributed to elastic scattering, a laboratory quarter-point angle of $\xi_{1/4} = 35.3 \pm 1.8^\circ$ and a total reaction cross section of $\sigma_R^{(1)} = 2.7 \pm 0.3$ b was determined for Reaction (1);

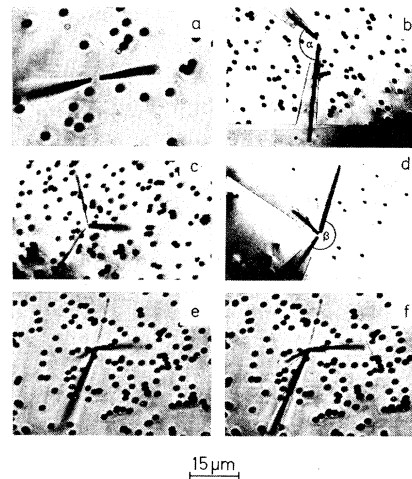


FIG. 1. Nuclear reactions as observed with a microscope. The black dots are due to bombarding heavy ions. The angle α is the angle between the projection of tracks onto the mica surface (i.e., the plane of observation) for two-pronged events ($\alpha \leq 180^\circ$). The angle β is similarly defined for three-pronged events; however, β is the largest angle between two neighboring tracks. (a) Two-pronged event due to binary reactions ($2F$), $\alpha > 165^\circ$; (b) two-pronged event due to sequential fission ($3F$), $\alpha \leq 165^\circ$; (c) three-pronged event due to sequential fission ($3F$), $\beta < 180^\circ$; (d) three-pronged event due to reactions with four fragments ($4F$), $\beta \geq 180^\circ$; (e), (f) four-pronged event due to reactions with four fragments ($4F$). In (a), (c), and (e) the focus is on the mica plane, thus giving a defocused picture for some parts of steep tracks. (b), (d), and (f) are composite pictures to show the tracks well in focus all the way. (a), (c), (e), and (f) are due to Reaction (1); (b) and (d) are due to Reaction (2).

for Reaction (2) we find $\xi_{1/4} = 40 \pm 4^\circ$ and $\sigma_R^{(2)} = 2.4 \pm 0.5$ b. The corresponding c.m. angles are $47.0 \pm 2.3^\circ$ and $61 \pm 5^\circ$, respectively. The methods for calculations are given elsewhere.⁹⁻¹¹

Here we discuss the events attributed to nuclear reactions and their classification in terms of observed fragment multiplicities, mostly for Reaction (1).⁹ 389 two-pronged events due to nuclear interactions were observed in Reaction (1). Typical examples are shown in Figs. 1(a) and 1(b). Events due to binary decay of the composite system have been selected by the following criteria: (1) Collinearity in the c.m. system, i.e., the angle α (defined in Fig. 1) between two tracks must be nearly π ($\alpha > 165^\circ$). The less than rigorous condition $\alpha > 165^\circ$ reflects the uncertainty in the angle measurement. (2) The measured track length l and angles ξ should nearly meet calculated track lengths l_{cal} and angles ξ_{cal} based on two-

body kinematics for the binary breakup of the composite system. Here, the total kinetic energy of the outgoing two fragments is assumed to correspond to complete damping of the kinetic energy of the relative motion in the entrance channel.

As our measurements are limited in accuracy ($\Delta l \leq 2 \mu\text{m}$; $\Delta \xi \leq 10^\circ$) and the range-energy relations used¹⁶ are known to be accurate only within 20%, we accepted all events in this class where the fragment mass ratio m_L/m_H is within the range $84/238 \leq m_L/m_H \leq 161/161$ and the total kinetic energy in the c.m. system is between 240 and 300 MeV.

26 out of 389 events fulfill criteria (1) and (2). Despite the limited accuracy [$\Delta(m_L/m_H) \leq 0.2$; $\Delta E \leq 20 \text{ MeV}$] we think that those events are of binary nature, or have at most a third partner of $m \leq 30 \text{ amu}$. Neutron and charged-particle emission are neglected. The total cross section for binary reaction ($2F$) is then $136 \pm 30 \text{ mb}$ in the 2π geometry, and gives the following lower limit on the total binary cross section (in 4π geometry) for Reaction (1): $\sigma_{2F}^{(1)} \geq 136 \pm 30 \text{ mb}$. Thus our results are in agreement with the radiochemical results of Ref. 5, that binary decay of a composite system is observed in Reaction (1). $(40 \pm 14)\%$ of $\sigma_{2F}^{(1)}$ is due to reactions yielding fragments in the mass range 140 to 180.

Events due to sequential fission can be recognized either directly or indirectly. As direct evidence we have the following: 98 three-pronged events are observed in Reaction (1) [see Figs. 1(c) and 1(d)]. 97 of those events with $\beta < 180^\circ$ are considered to be due to sequential fission, while the remaining one event with $\beta \geq 180^\circ$ will be discussed later (β is defined in Fig. 1). As indirect evidence we have the following: 235 two-pronged events do not show collinearity ($\alpha \leq 165^\circ$) [see Fig. 1(b)]. Because of momentum conservation, they are considered to be due to sequential fission with a third fragment $m > 30 \text{ amu}$, emitted at an angle not accessible to our 2π geometry. The limit $\alpha \leq 165^\circ$ is somewhat arbitrary, but it has been shown that track-length (l) and angular (ξ) distributions of these events are similar to those observed as direct three-pronged events.¹³ This yields the following lower limits for sequential fission ($3F$) in the 4π geometry for Reactions (1) and (2), respectively:

$$\sigma_{3F}^{(1)} \geq 1640 \pm 150 \text{ mb} = (0.61 \pm 0.05)\sigma_R^{(1)},$$

$$\sigma_{3F}^{(2)} \geq 2460 \pm 480 \text{ mb}.$$

This large contribution is in agreement with radio-chemical results: The components ($B/2$) and ($D/2$), as defined in Ref. 5 give $\sigma_{3F} = (0.51 \pm 0.08)\sigma_R$ for the interaction of 605-MeV Kr with a thick uranium target.

This large contribution of sequential fission is due to more or less inelastic collisions of the Kr ion with an uranium nucleus, followed by a binary decay of the excited uranium nucleus, as can be shown in a qualitative manner by the observed angular and track-length distributions of 97 three-pronged events [Figs. 2(a)–2(c)]. Here, the distributions of the longest track and two shorter tracks in each individual three-pronged event are shown separately [Fig. 2(b)]. One observes always one rather long track and two short tracks. The long tracks are rather well focused around the quarter-point angle $\xi_{1/4}$ [Fig. 2(a)], and we associate them with “projectilelike” ions; they can be as long as tracks from 800-MeV Kr ions (64 μm). The two short tracks are similar in length to fission tracks from $U(n, f)$ reactions,

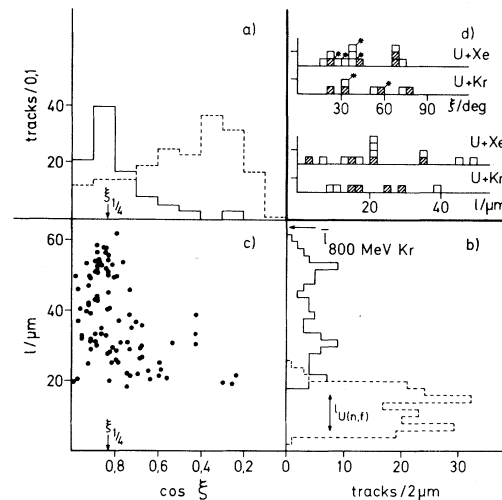


FIG. 2. (a) Distribution of the angle ξ between track and beam direction for three-pronged events due to sequential fission [Reaction (1)]. The distribution of the longest track (solid line) in each event is shown separately from the distribution of the two shorter tracks of each event (dashed line). The experimental cutoff for the registration of tracks is at $\cos \xi \approx 0.1$. (b) Distribution of the track length l for the same events (solid line, the longest track; dashed line, the two shorter tracks). (c) Correlated representation of the longest track and its angle ξ for these three-pronged events. (d) Distribution of l and ξ for events due to reactions with four fragments (open areas: $4F$ indirect; hatched areas: $4F$, direct). Asterisks indicate the ξ for the longest track. Each square represents one track.

TABLE I. Number of observed events due to reactions with four fragments. $N(4F)$ is the number of events due to reactions with four fragments (direct: four-pronged events in the 2π geometry; indirect: three-pronged events in the 2π geometry with $\beta \geq 180^\circ$). $N(3F)$ is the number of three-pronged events (in the 2π geometry) due to sequential fission.

| Reactions | $N(4F)$ | | $N(4F)/N(3F)$ |
|---|---------|----------|-----------------------------------|
| | Direct | Indirect | |
| (320–400)-MeV $^{40}\text{Ar} + \text{U}$ | 0 | 0 | $0/500 = 0$ ^a |
| 540-MeV $^{56}\text{Fe} + \text{U}$ | 0 | 1 | $1/100 \approx 0.01$ ^b |
| 800-MeV $^{84}\text{Kr} + \text{U}$ | 1 | 1 | $2/97 \approx 0.02$ ^c |
| 1080-MeV $^{136}\text{Xe} + \text{U}$ | 1 | 3 | $4/100 \approx 0.04$ ^c |

^aRefs. 2 and 13.

^bRef. 14.

^cThis work.

as indicated in Fig. 2(b); additionally, they are distributed nearly isotropically in space [Fig. 2(a)]. So we interpret our three-pronged events as being due to inelastic collisions where the “projectilelike” ion is scattered at angle around $\xi_{1/4}$ —as has been observed in counter experiments—while the excited heavy fragment undergoes fission. Figure 2(c) shows the angle ξ and track length l of only the longest track for three-pronged events in a correlated form: For the limited number of events available we think that the clustering at $\xi_{1/4}$ for relatively long tracks ($\sim 50 \mu\text{m}$) is possibly due to a rather short interaction time between Kr and U, while the broader angular distribution for relatively short tracks ($\sim 25 \mu\text{m}$) is possibly due to longer interaction times. The continuous transition from relatively long tracks down to relatively short tracks indicates a rather smooth distribution of energies damped during the heavy-ion collisions. However, our analysis does not allow any conclusion on whether or not we have seen any “ternary fission” events, as postulated recently by Diehl and Greiner for such heavy systems.¹²

Figures 1(e) and 1(f) give an example of a four-pronged event. The probability of an accidental overlap of two binary events is $< 10^{-5}$. Figure 1(d) gives an example of a three-pronged event with $\beta \geq 180^\circ$. Because of momentum conservation, at least one more reaction partner was produced but not registered with our geometric arrangement. Such events are also considered as being due to reactions with four fragments. Table I gives a summary of reactions with four fragments ($4F$) in heavy-ion-induced reactions. Ions heavier than Ar are needed to induce this novel decay channel. For Kr- and Xe-induced re-

actions the lower limits on the cross sections are

$$\sigma_{4F}^{(1)} \geq 8 \pm 6 \text{ mb} \approx 0.003\sigma_R^{(1)},$$

$$\sigma_{4F}^{(2)} \geq 40 \pm 20 \text{ mb} \approx 0.016\sigma_R^{(2)},$$

for Reactions (1) and (2), respectively. For the sake of completeness, the distributions of l and ξ for all events with four fragments are shown in Fig. 2(d). Because of the small number of events observed, it appears to be premature to discuss the reaction mechanism involved in the framework of recent theoretical considerations by Möller and Nix.¹⁵

We thank Professor I. S. Grant (Manchester) and Dr. H. Grunder (Berkeley) for arranging the irradiations, and Dr. J. Péter (Orsay) and Professor W. Greiner and his co-workers (Frankfurt) for stimulating discussions. Financial support by the Bundesministerium für Forschung und Technologie, Bonn, and by the Gesellschaft für Schwerionenforschung, Darmstadt, is appreciated.

^(a)Present address: Gesellschaft für Schwerionenforschung, D-6100 Darmstadt, Germany.

¹R. L. Fleischer, P. B. Price, R. M. Walker, and E. L. Hubbard, Phys. Rev. **143**, 943 (1966).

²R. Brandt, Angew. Chem. **83**, 1000 (1971); for a review, see H.-J. Becker, P. Vater, R. Brandt, A. H. Boos, and H. Diehl, Phys. Lett. **50B**, 445 (1974).

³K. L. Wolf, J. P. Unik, J. R. Huizenga, J. Birkelund, H. Freiesleben, and V. E. Viola, Phys. Rev. Lett. **33**, 1105 (1974); J. P. Bondorf, J. R. Huizenga, M. I. Sobel, and D. Sperber, Phys. Rev. C **11**, 1265 (1975).

⁴U. Reus, A. M. Habbestad-Wätzig, R. A. Esterlund, P. Patzelt, and I. S. Grant, Phys. Rev. Lett. **39**, 171 (1977).

⁵J. V. Kratz, A. E. Norris, and G. T. Seaborg, Phys. Rev. Lett. **33**, 502 (1974).

⁶R. J. Otto, M. M. Fowler, D. Lee, and G. T. Seaborg, Phys. Rev. Lett. **36**, 135 (1976).

⁷J. Péter, C. Ngô, F. Plasil, B. Tamain, M. Berlinger, and F. Hanappe, private communication.

⁸P. Vater, H.-J. Becker, and R. Brandt, J. Radioanal. Chem. **32**, 275 (1976).

⁹P. Vater, dissertation, Philipps-Universität, Marburg, 1976 (unpublished).

¹⁰J. R. Birkelund, J. R. Huizenga, H. Freiesleben, K. L. Wolf, J. P. Unik, and V. E. Viola, Jr., Phys. Rev. C **13**, 133 (1976).

¹¹H.-J. Becker, dissertation, Philipps-Universität, Marburg, 1977 (unpublished).

¹²H. Diehl and W. Greiner, Nucl. Phys. **A229**, 29 (1974).

¹³V. P. Perelygin, N. H. Shadieva, S. P. Tretiakova, A. H. Boos, and R. Brandt, Nucl. Phys. **A127**, 577 (1969).

¹⁴P. Vater, H.-J. Becker, and R. Brandt, Radiochem. Radioanal. Lett. **19**, 87 (1974).

¹⁵P. Möller and J. R. Nix, Nucl. Phys. **A272**, 502 (1976).

Fine Structure of the Magnetic Dipole Giant Resonance in ²⁰⁸Pb

S. Raman, M. Mizumoto,^(a) and R. L. Macklin

Oak Ridge National Laboratory, Oak Ridge, Tennessee 37830

(Received 23 May 1977)

Eighteen $M1$ transitions to the ²⁰⁸Pb ground state have been identified and their radiative widths measured in a study of the reaction ²⁰⁷Pb(n, γ) combined with the results from recent neutron transmission and elastic scattering measurements. In the excitation region between 7.37 and 8.23 MeV, $\sim 50\%$ of the expected total $M1$ strength in ²⁰⁸Pb has been located.

In a simple shell-model picture,¹⁻³ two 1^+ states are expected in ²⁰⁸Pb at ~ 7 MeV resulting from the one-particle, one-hole (1p-1h) configurations $\nu(i_{13/2}^{-1}, i_{11/2})$ and $\pi(h_{11/2}^{-1}, h_{9/2})$. These states are expected³ to nearly exhaust a transition strength of $B(M1) \uparrow \approx 36 \mu_0^2$. The inclusion of 2p-2h configurations^{4,5} results in the splitting of these two states into many components. Several measurements have been carried out to locate this $M1$ strength. In the unbound region, the techniques have been primarily angular distributions,⁶⁻⁸ and polarization measurements⁹⁻¹¹ in the (γ, n) reaction. In the bound region, there have been resonance fluorescence measurements¹² and particle- γ directional-correlation measurements utilizing the ($p, p'\gamma$) and ($d, d'\gamma$) reactions.¹³ At present, the overall experimental situation concerning the location of the $M1$ strengths is very unclear because many of the previous claims have not withstood subsequent scrutiny.⁶⁻¹³ In particular, the original claim⁶ of finding a large concentration of $M1$ strength spread over seven states in the 7.4-8.3-MeV excitation region has been whittled away to the extent that a recent Letter¹¹ states that the only significant 1^+ strength in this region occurs in a single state, although three others, previously unresolved, have small 1^+ components. We will show that this is not the case. However, only three of the seven original 1^+ assignments remain intact. In a new approach, we have studied the

reaction ²⁰⁷Pb(n, γ) at the Oak Ridge Electron Linear Accelerator (ORELA) in the neutron energy region up to 1 MeV (7.4-8.4-MeV excitation energy). We have obtained absolute radiation widths for a large number of dipole transitions to the ²⁰⁸Pb ground state. Eighteen transitions were identified as $M1$ on the basis of parity assignments from recent neutron transmission and scattering measurements¹⁴ also carried out at ORELA and from polarization measurements at Argonne.^{9,11} We have located nearly half of the expected total $M1$ strength in ²⁰⁸Pb. Our results are expected to influence future theoretical calculations of this strength significantly.

Prompt γ -ray emission from a 92.4%-enriched 249-g ²⁰⁷Pb metal target was detected at 40 m from the ORELA pulsed neutron source as illustrated by Macklin and Allen.¹⁵ To minimize sensitivity to scattered neutrons, fluorocarbon-based liquid scintillators were used with a bias set just above the 197-keV, second inelastic γ ray from ¹⁹F (the threshold for the third is above 1.4 MeV). The sensitivity itself was evaluated with a sample of ²⁰⁸Pb which has very few resonances. The observed pulse height and time-of-flight information was transformed¹⁶ to neutron captures per sample nucleus as a function of neutron energy. The observed resonance peaks were fitted with single-level parameters by a least-squares computer code¹⁷ which takes into account effects such

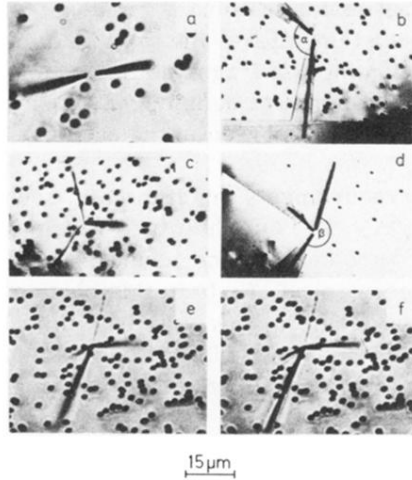


FIG. 1. Nuclear reactions as observed with a microscope. The black dots are due to bombarding heavy ions. The angle α is the angle between the projection of tracks onto the mica surface (i.e., the plane of observation) for two-pronged events ($\alpha \leq 180^\circ$). The angle β is similarly defined for three-pronged events; however, β is the largest angle between two neighboring tracks. (a) Two-pronged event due to binary reactions ($2F$), $\alpha > 165^\circ$; (b) two-pronged event due to sequential fission ($3F$), $\alpha \leq 165^\circ$; (c) three-pronged event due to sequential fission ($3F$), $\beta < 180^\circ$; (d) three-pronged event due to reactions with four fragments ($4F$), $\beta \geq 180^\circ$; (e), (f) four-pronged event due to reactions with four fragments ($4F$). In (a), (c), and (e) the focus is on the mica plane, thus giving a defocused picture for some parts of steep tracks. (b), (d), and (f) are composite pictures to show the tracks well in focus all the way. (a), (c), (e), and (f) are due to Reaction (1); (b) and (d) are due to Reaction (2).